catalysts

MDPI

Article

Antibacterial Activity Assessment of $Bi_2WO_6/Ag_3PO_4/Ag$ Photocatalyst and *Persian Oak fruit* Phytobiotic

Mohsen Azizi [1], Kheibar Dashtian [2], Fereshteh Amourizi [2], Asghar Sharifi [1,*], Mehrorang Ghaedi [2,*], Vahid Pezeshkpour [1,3], Arsalan Azizi [4], Shapor Aghaee [5], Seyed Abdolmajid Khosravani [1] and Ghulam Yasin [6]

1 Cellular and Molecular Research Center, Yasuj University of Medical Sciences, Yasuj 75914-93686, Iran
2 Department of Chemistry, Yasouj University, Yasuj 75918-74831, Iran
3 Dena Pathobiology Laboratory, Department of Biotechnology and Microbial Nanotechnology, Yasuj 75918-74831, Iran
4 Pathology Group, Yausj University of Medical Sciences, Yasuj 75914-93686, Iran
5 Department of Internal Medicine, Yausj University of Medical Sciences, Yasuj 75914-93686, Iran
6 Institute for Advanced Study, Shenzhen University, Shenzhen 518060, China
* Correspondence: asgharsharifi@yahoo.com (A.S.); m_ghaedi@mail.yu.ac.ir (M.G.); Tel./Fax: + 98-743-333-7251 (A.S.)

Abstract: The antibacterial effect of the previously reported $Bi_2WO_6/Ag_3PO_4/Ag$ Z-scheme heterojunction photocatalyst compared with a phytobiotics named, aqueous extract of *Persian Oak fruit*. The impact of both materials on the expression of the *urease gene* was checked in two kinds of samples such as clinical and standard *Helicobacter pylori* (*H. pylori*). The gene expression differences were collected by real-time PCR from clinical strains and the standard of *H. pylori* as well as the MIC and MBC were found to be 3.1 and 0.8 mg/mL, and 6.2 and 1.6 mg/mL, for $Bi_2WO_6/Ag_3PO_4/Ag$ photocatalyst and *Oak fruit* Phytobiotics, respectively. Due to the impact of *Oak fruit* extract on the *urease gene* of *H. pylori*, it is possible to use it as a disinfector against this bacterium and the proposed photocatalyst, for efficiently purifying *H. pylori* bacteria from contaminated environment.

Keywords: *Helicobacter pylori*; phytobiotic; antibacterial photocatalyst; *Persian Oak fruit* extract; $Bi_2WO_6/Ag_3PO_4/Ag$

Citation: Azizi, M.; Dashtian, K.; Amourizi, F.; Sharifi, A.; Ghaedi, M.; Pezeshkpour, V.; Azizi, A.; Aghaee, S.; Khosravani, S.A.; Yasin, G. Antibacterial Activity Assessment of $Bi_2WO_6/Ag_3PO_4/Ag$ Photocatalyst and *Persian Oak fruit* Phytobiotic. *Catalysts* **2022**, *12*, 1027. https://doi.org/10.3390/catal12091027

Academic Editor: Omid Akhavan

Received: 13 July 2022
Accepted: 4 September 2022
Published: 9 September 2022

1. Introduction

A significant challenge in today's world is health disparities that cause by many factors for humankind in developing countries, such as; the level of economic stability, physical environment, health care system, food, and water healthy options [1]. Reaching equal right in health for people around the world need the double effort of scientist on each mentioned above category. A huge amount of research annually takes place in bacteria-related infection and contamination have been threatening human health since the ancients to achieve this goal, is simple, and on a budget way for the treatment of food resources in remote areas that are affected by bacterial infection is a priority [2]. One of the main subcategories in this area is the contamination of pathogenic bacteria that endanger drinking water safety; statistics show an increasing water shortage, and many communities have to use drinking water from reservoirs containing various pathogenic bacteria [3]. Hence, disinfection of pathogenic bacteria contaminations is one of the ideal choices for increasing water quality as well as people's living standards [4]. *H. pylori* is a harmful risk source in drinking water and human health; which categorized as a spiral-shaped bacterium and gram-negative, that starts colonization in the stomach and neutralizes the acidic conditions and, moves towards the host gastric epithelium and binds to the host cell receptors that is the causal agent for prevalent gastric diseases [5]. To meticulously examine the function of *H. pylori* researchers, focus on urease as a constructive agent of human gastritis that catalyzes the hydrolysis of urea to yield NH_3 and CO_2 [6]. Although, this enzyme makes a convenient place for this

acid-sensitive organism in the gastric mucosa, the NH_3 produced by hydrolysis of urea can also produce severe cytotoxic effects within the gastric epithelium. To solve this problem of health inequity, there are two main categories; the first includes disinfection technologies in the water before the bacteria can enter the human body, and the second is after the infection of humans, with patient treatment by antibiotic drugs. To deal before humans face waterborne pollution, one of the proposed actions for *H. pylori* is photocatalytic water disinfection which has been studied for the inactivation of pathogens with eco-friendly material and a simple visible light radiation [7]. To reach, this attitude, noble metal-modified photocatalysts such as silver captured extensive attention due to promoting photocatalytic activity [8,9]. The combination of electron pairs and photo-generated hole through the formation of the Schottky junction is hampered by sinking electrons with silver, which helps to strengthen the light absorption via the surface plasmon resonance (SPR) effect [10]. In this regard, silver as a noble metal constructs heterogeneous photocatalyst coupled with a metal oxide to improve its photocatalytic activity and the poor utilization of visible light absorption [11,12]. Therefore, developing a Z-scheme photocatalyst that mimics the natural photosynthesis system shows promise, including spatially separated reductive and oxidative active sites and well-preserved strong redox ability, which would benefit the photocatalytic performance, along with a special spectrum of light; this could significantly improve the efficiency of visible-light-driven disinfection [13,14]. Another preventive measure is phytobiotics for water disinfection [15], as therapeutic regimes after infection have failed in many areas, due to the increasing resistance to key antibiotics and the increase in this global problem [16]. Phytobiotics are a common alternative to sterilizing for *H. pylori* infection, which is as old as human beings [17]. In the past few years, there has been a growing relevance in the alternative therapy category, particularly the utilization of an herbal products are prepared from the medical plants for purification of water supplements [18]. The category of phytobiotics benefits from no side effects of chemical material and is more useful for people in any situation. The investigation of the new pharmacologically active agents over the screening of various plant extracts led to safe disinfectors, which is known as phytochemical constituents [19]. Herein, we studied a previously reported $Bi_2WO_6/Ag_3PO_4/Ag$ Z-scheme plasmonic heterojunction driven blue-light photocatalyst for a novel application in this paper as an antibacterial photocatalyst, and compared it with Oak fruit*'s* extract impact on the *urease gene* of *H. pylori* expression. The optical properties, surface morphology and crystalline structure of photocatalysts have been studied through various characterizations. Furthermore, the $Bi_2WO_6/Ag_3PO_4/Ag$ and *Oak fruit* were applied for the disinfection of biopsy samples from *H. pylori* bacteria under the clinical and standard conditions as confirmation of antibacterial effect.

2. Results and Discussion

2.1. Characterization of Prepared Samples

In our previous report, we verified the novel $Bi_2WO_6/Ag_3PO_4/Ag$ Z-scheme heterojunction photocatalyst structure in detail, with XRD, FE-SEM, UV-Vis DRS, PL, Tauc plot, and FT-IR spectra [8].

2.2. Photocatalytic Inactivation Mechanism

The antibacterial performance of the obtained photocatalyst and Oak fruit*'s* extract was investigated by inactivation of *H. pylori* under blue light and standard conditions for bacteria for estimating the potential of these two proposed substances for their important disinfection application in the contaminated microbial environment (see Figure 1) [1,2]. Before adding any photocatalyst the sensitivity of *H. pylori* under blue light is determined, and their activities, do not change significantly, and light irradiation has a minor effect on inactivating.

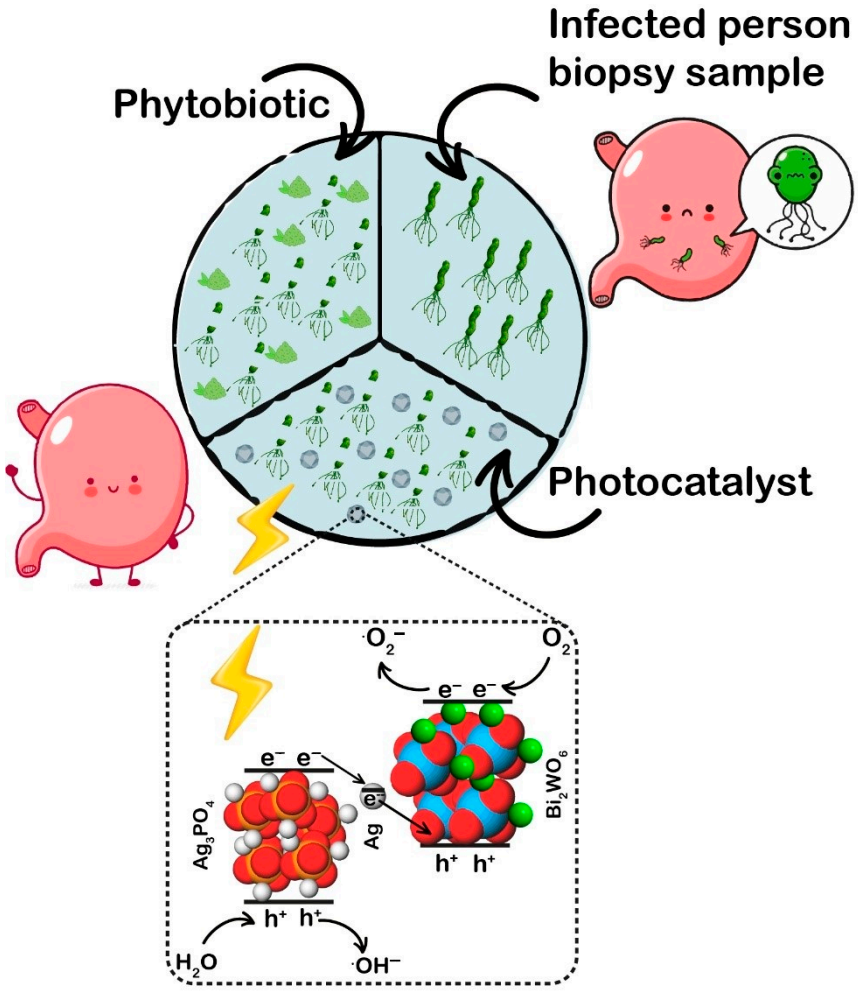

Figure 1. Schematic illustration of photocatalytic and phytobiotics disinfection by $Bi_2WO_6/Ag_3PO_4/Ag$ and *Oak fruit* extract.

After photocatalyst addition, it is observed that after 1080 Min. In the presence of a mixt of Bi2WO6/Ag3PO4/Ag and *Oak fruit*'s Extract, with irradiation with blue-light, the *pylori* was inactivated. This was likely due to the rapid recombination of photogenerated holes and electrons.

Herbal disinfectors are another method proposed for disinfection; *Oak fruit* antimicrobial activities of conventional antimicrobials are hinged on inhibition of cellular functions and structure, including cell membrane function,, and act by collapsing cell walls and membranes, resulting in the leakage of the *H. pylori* component, interrupting the proton motive force and dysfunction of the efflux pump and enzymes.

2.3. MIC and MBC Results

To determine the MIC of Bi2WO6/Ag3PO4/Ag as a novel photocatalyst under the light and *Oak fruit* extract, the antibacterial broth method used in the plates had 96 parts based on the CLSI 2015 standard. The average MIC was calculated for the*H. pylori* standard strain (ATCC 26695) and clinical strains in Figure 2. According to the MIC results, the minimal concentration of MBC was determined. Two-parts pre and two parts post growth of the bacteria stopped growing microaerobic conditions on blood agar, and at 37 °C for five days on the plate. Subsequently, concentrations without bacterial growth were observed as MBC. Each test was repeated three times and the average results are shown in the Figure 2 [20,21]. Each test was repeated three times, and the average results are shown in Table 1.

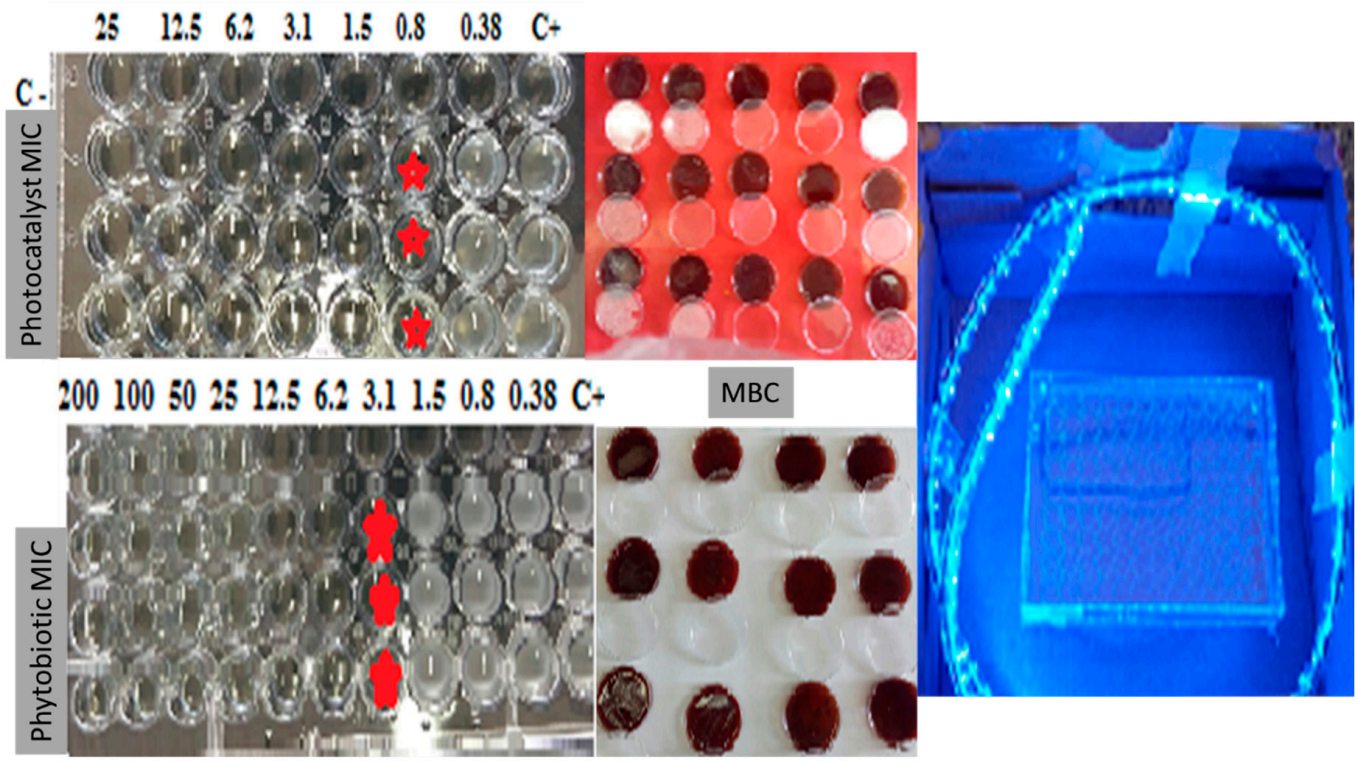

Figure 2. MIC and MBC for *H. pylori* (ATCC 26695), (red stars = calculated MIC for photocatalyst and phytobiotic.).

Table 1. The MIC of extracted *Oak fruit*, $Bi_2WO_6/Ag_3PO_4/Ag$ and mixed them against the *H. pylori* (ATCC 26695) and *H. pylori* clinical strain.

Bacterial Strain	*Oak fruit* (mg/mL)	$Bi_2WO_6/Ag_3PO_4/Ag$ (mg/mL)	Mixed (mg/mL)	
			Oak fruit	$Bi_2WO_6/Ag_3PO_4/Ag$
H. pylori (ATCC 26695)	3.1	0.6	1.55	0.3
Clinical strain	3.1	0.8	3.1	0.8

2.4. PCR for Various Gene Confirmations

Urease and gyrB gene expression were determined by a real-time PCR system (Applied Biosystems, Foster City, CA, USA). Use SYBR Green Master Mix (Table 2). The reaction volume was 20 mg and contained 2.5 mg cDNA, 0.5 mg of each primer (10 pg/mg), 10 mg of master mix, and 6.5 mg of double distilled water. The sequences and melting temperatures of the genes examined (urease A and gyrB) are shown in Table 3 [22]. Thermal cycling included an initial denaturation at 95 °C for 15 min, followed by 38 cycles of denaturation at 95 °C for 15 s, annealing at 60 °C for 30 s, and extension at 72 °C for 40 s (Table 4). As a stable gene in different situations, gyrB was used as an internal control (housekeeping gene) to compare and validate gene expression. Each sample was reacted three times, and the average value obtained was used as the gene expression level of the sample. For relative measurement of the tests, the calculation was made based on $e^{-\Delta CT}$, the efficiency of each target and reference gene calculated from the standard curve. Efficiency was considered equal to "2" because both tests were nearly perfect.

2.5. Evaluation of Real-Time PCR

Evaluation of primer-dimers and other artifacts was done by melting curve analysis. Finally, only dimer- and artifact-free reactions were validated. Outcomes were read with the 'second derivative maximum' algorithm of the software provided. The Light Cycler

software starts the standard curve by plotting 'the crossing cycle number' versus logarithms of the provided concentrations for all controls. Ultimately, a regression line was drawn between these points. The software calculated the concentrations of the studied genes with the aid of this standard curve (Figure 3).

Table 2. Used compounds for PCR reaction.

Compounds	Concentration
Master mix	12.5 mg (1×)
Distill water	9.0 mg
Template	2.5 mg (20pg)
Primer forward	0.5 mg (10 µM)
Primer reverse	0.5 mg (10 µM)

Table 3. Sequence and melting temperature of urease and gyrB genes, with primer size used in Quantitative Real-Time PCR method.

Primer	Sequence	Amplicon (bp)	Tm
Urease-F	′5-GCCAATGGTAAATTAGTT-3′	245	58
Urease-R	′5-CTCCTTAATTGTTTTTAC-3′		58
gyrB-F	′5-GACCCGTACGCTAAACAAC-3′	110	63.3
gyrB-R	′5-AGAAATAACCGCAATCAGG-3′		66.4

Table 4. Conditions of PCR reaction.

Gene	Initial Denaturation	Secondary Denaturation	Primer Connecting	Primer Duplication	Final Duplication
Urease A	95	95	60	72	72
	15 min	15 s	30 s	40 s	7 min

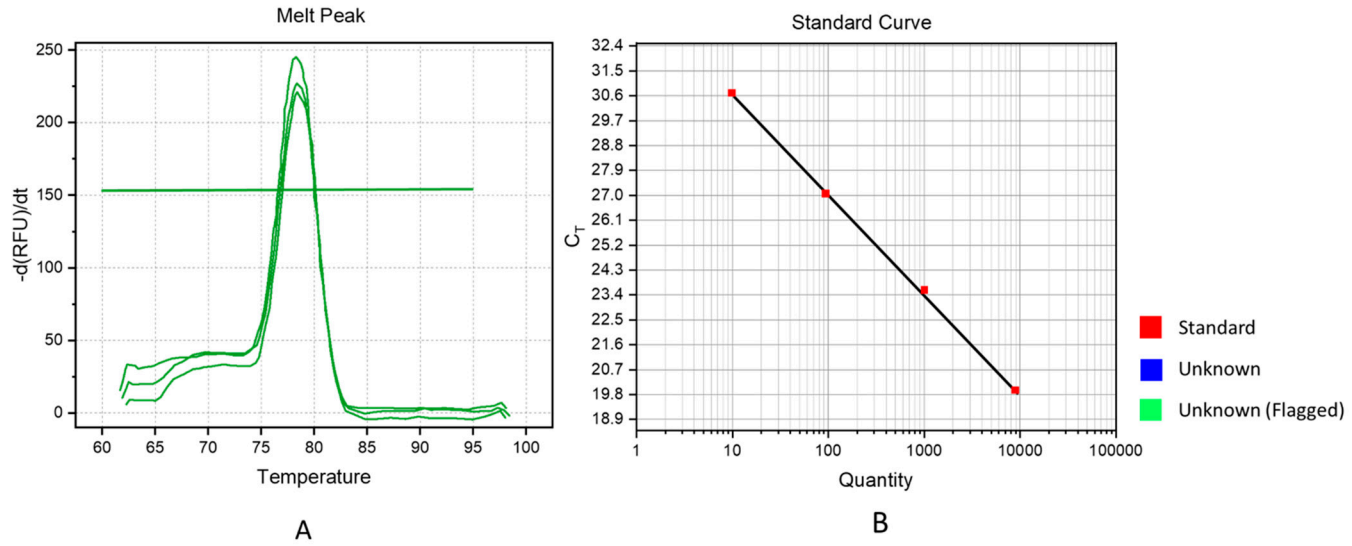

Figure 3. qPCR using the primer DNA gyrase: melting curve peaks (**A**) and standard curve (**B**); all peaks were at 65 for the detection of DNA gyrase B gene in the strains of *H. pylori.*

2.6. PCR to Determine Urease Gene

The *urease gene* was confirmed by using the kit of Sin a gene Company of America–referring to their tables. The presence of the *urease gene* was established between PCR, and

five samples of *H. pylori* with the *urease gene* were selected (Table 5). shows the outcomes of the PCR molecular method to confirm the presence of the *urease gene* in standard, and clinical *H. pylori*. All strains had the Urease gene.

Table 5. The percentage of expression of urease A gene in MIC concentration in *H. pylori* strains was studied in the presence of Extract of *Oak fruit*, Nano-structure of the $Bi_2WO_6/Ag_3PO_4/Ag$ mixed $Bi_2WO_6/Ag_3PO_4/Ag$.

Type of Intervention \ Strain Studied	Extract of *Oak fruit* in Concentration MIC	$Bi_2WO_6/Ag_3PO_4/Ag$ in Concentration MIC	Mixed *Oak fruit* Extract and $Bi_2WO_6/Ag_3PO_4/Ag$ in Concentration MIC
***H. pylori* (ATCC 26695)**	0.06%	0.53%	31%
Average of gene expression for 5 Clinical strains	11%	9%	42%

2.7. Determination of the Amount of the Urease Gene Expression in the Presence of the Photocatalyst and the Oak fruit *Extract*

Based on the gene expression according to Figure 4 using the PFAFFL method to regulate the quantity of *urease gene* expression. In this method, it is assumed that the sample efficiency and internal control were 99%, and the formula $2^{(-\Delta CT)}$ was used to evaluate the gene expression.

$$\text{Ratio} = \frac{(\text{E target})^{\Delta CT \text{ target (control}-\text{sample)}}}{(\text{E ref}^{\Delta CT \text{ ref (control}-\text{sample)}}}$$

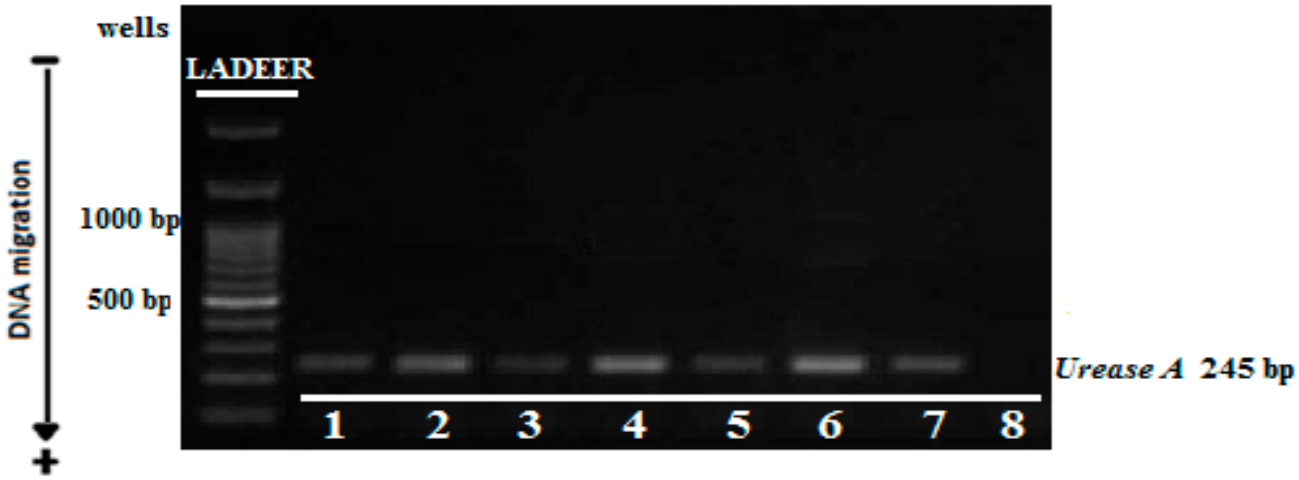

Figure 4. The result of the electrophoresis of *urease gene* PCR products on agarose gel. Lader: (100 bp); 1: the presence of the *urease gene* in *H. pylori* (ATCC 26695) (C+); 2–7: the presence of the *urease gene* in *H. pylori* clinical strains; 8: absence of the *urease gene* in *H. pylori* clinical strains that were negative for the urease test (C−).

2.8. Comparison of the ZOI of the Treatments

Appearance comparison of inhibition zone of *H. pylori* strains in the presence of study analysis with ZOI of selected antibiotics and the result of most studied strains (Figure 5). The results showed the antimicrobial effect of *Oak fruit* extract compared to standard antibiotics such as tetracycline, metronidazole, and amoxicillin by the disk diffusion method was close to tetracyclic (Figure 6).

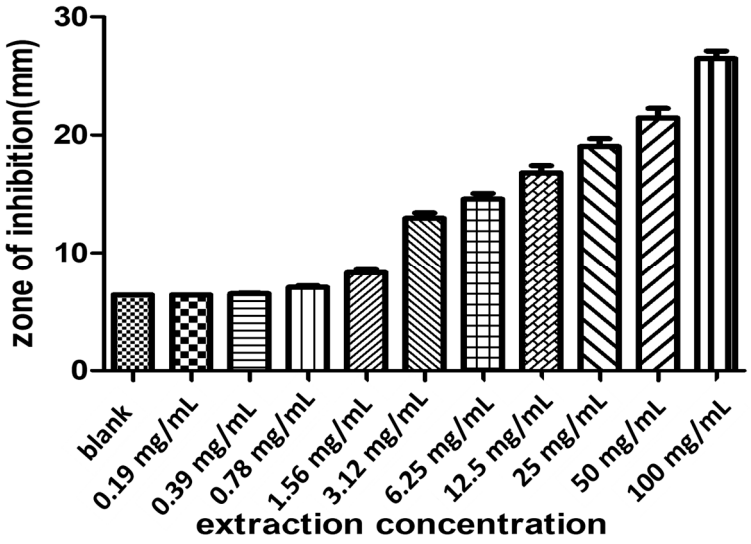

Figure 5. Comparison of the ZOI of the treatments of extract of *Oak fruit*.

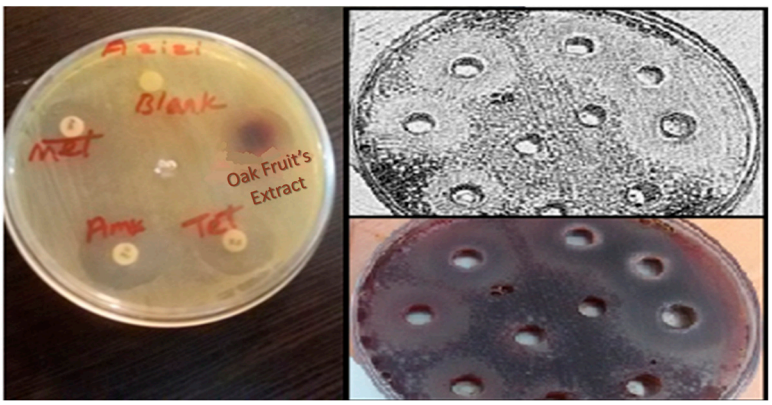

Figure 6. The inhibition zone of extract of *Oak fruit* for antibacterial activity using disc diffusion method and Agar well diffusion method.

3. Materials and Methods

3.1. Reagents

100 consecutive untreated patients undergoing upper gastroduodenal endoscopy at the Dr. Azizi clinical laboratory (the Kohgiluyeh and Boyer-Ahmad Province, Iran) were included in the study. As well as, clinical samples, *H. pylori*'s standard strain was also used; The results of the PCR molecular method confirm the presence of the *urease gene* in standard and clinical *H. pylori*. Sterile cotton in a semisolid agar transport medium (Portagerm; bioMe´rieux, Marcy l'Etoile, France) was chosen for biopsy specimens and samples were dipped in culture examination as microbiology standard methods (such as gram stain, catalase, oxidase and urease tests), are shown in (Figures 7 and 8). An extra antrum biopsy specimen for PCR analysis was obtained. For culture and PCR biopsy until processing, specimens were kept at −70 °C. The endoscopic apparatus (Olympus GIF-IT or Fujinon UGIF-P2), including all channels and biopsy forceps, was cleaned and sterilized by immersion in two percent Glutardialdehyde (Cidex; Surgikos Ltd., Livingstone, Scotland) solution for 15 min, soak in water, and dried after every single usage by patient and either at the end of each endoscopic session. In addition, the standard strain of *H. pylori* (American Type Culture Collection: 26695, Pasteur Institute, Tehran, Iran) was used as case study bacteria. Bismuth nitrate pentahydrate, ethanol, acetic, sodium tungstate dehydrate, polyvinylpyrrolidone, Silver nitrate, sodium borohydride, were purchased from Merck Company, Darmstadt, Germany. All equipment, software, and chemical reagents were used according to the manufacturers' guidelines, as detailed in our previous publications [8,20].

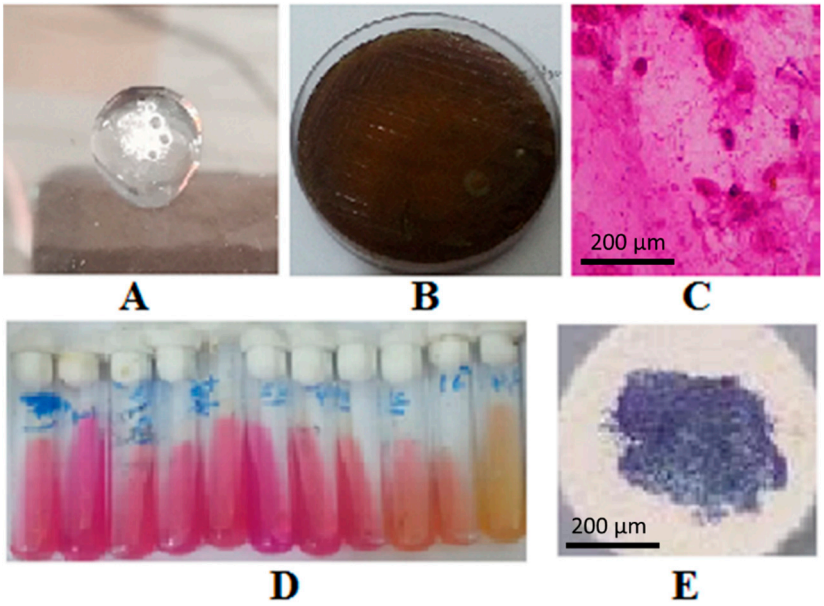

Figure 7. *H. pylori* Bacterial Diagnostic Tests Catalase (**A**), Positive culture on selected culture media of Columbia blood agar (**B**), Curved Bacillusand Gram-negative (**C**), Urea test (**D**) and Positive oxidase test (**E**).

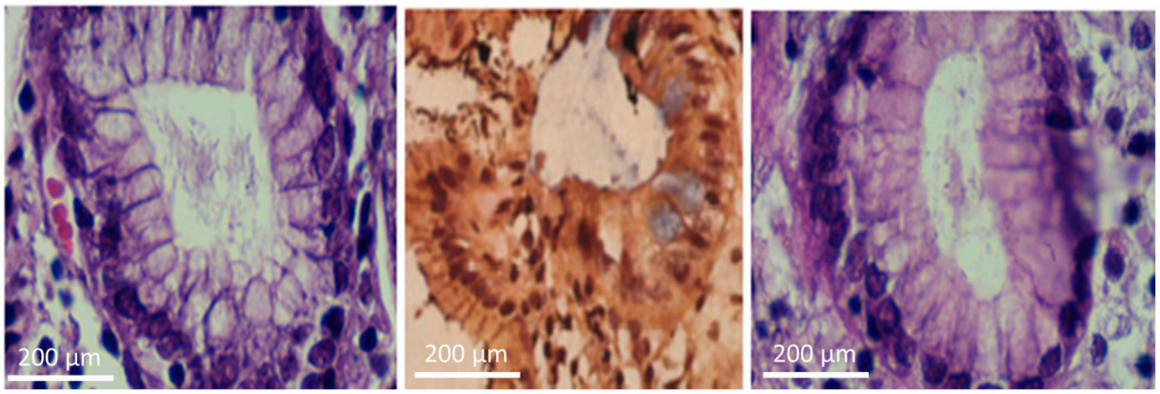

Figure 8. Antral mucosa showing with high-power photomicrograph with focal intestinal metaplasia (goblet cells stained with alcian blue at pH 2.5), heavy *H. pylori* infection (spiral bacteria stained dark brown with a modified Steiner stain) the organism is concentrated within the superficial mucus overlying epithelial cells. The gastric antral biopsy is preferred for evaluating of *H. pylori* gastritis, and moderate inflammation.

3.2. $Bi_2WO_6/Ag_3PO_4/Ag$ Photocatalyst Preparation

The $Bi_2WO_6/Ag_3PO_4/Ag$ was prepared according our previous work as follows [8]: Briefly, for Bi_2WO_6 synthesis one gram of PVP and one mmol of $Bi(NO_3)_3$ $5H_2O$ were added to a mixture ratio 3:1:1 of DI water, ethanol, and acetic acid and then placed for 20 min under an ultrasonic probe. After that, a solution containing 0.5 mmol of Na_2WO_4 in five mL of DI water was added to the solution and ultrasonicated for more than 30 min. The resulting solution was then placed in a stainless-steel, PTFE-lined autoclave at temperature of 180 °C overnight. The obtained powder cooled and washed continuously with ethanol and DI water mixture and dried overnight.

In the next step, 0.2 g ofBi_2WO_6 was added to 100 mL of DI water for 30 min under ultrasonication. Then, 0.5 g of PVP and 0.15 g of $AgNO_3$ were added to the solution and were ultrasonicated for over an hour. To reduce the Ag^+ ions to the Ag, 100 µL of $NaBH_4$ 10^{-3} mol L^{-1} was added and the obtained solution was ultrasonicated for 30 min. At last, 0.33 g Na_2HPO_4 for the reaction between the excess Ag^+ ions with anion PO_4^{3-}, added to

the suspension, for Ag_3PO_4 formation. The final $Bi_2WO_6/Ag_3PO_4/Ag$ photocatalyst was separated by centrifugation and washed and then dried for further application.

3.3. Culture

Gastric biopsy samples were ground at 10,000 for 15 s with an electric tissue homogenizer (Ultraturrax, Iena, Germany) and soon after inoculated onto selective Columbia blood agar and incubated under microaerophilic (5% O_2, 10% CO_2, and 85% N_2) conditions at 37 °C for up to seven days [23,24].

3.4. Oak fruit's Extraction

Firstly, the inner shell of *Oak (Jaft)*, with the help of a native instrument name ronjok (Figure 1A), was separated and dried, then powdered and kept for further use in a dark place. After that, 100 g of dry sample is put into a suitable container and mixed with 1000 mL solution (chloroform, ethanol 80%, and acetone), for ultrasonic extraction. Lastly, the solution was centrifuged and filtered at 3000 rpm for 10 min. The extraction was evaporated by rotary evaporator to dryness at a temperature lower than 40 °C and the residue was kept at 4 °C for further uses (see Figure 9) [25]. FTIR spectroscopic studies were carried out to find out the possible chemical present in the extract. The broad and narrow peaks of the fruit extract shown in Figure 1 part C. The peak at about 3300 cm^{-1} belongs to O–H stretch and the band at about 2900 cm^{-1} indicates the H–C–H symmetric stretching of alkanes. The band at about 1000 cm^{-1} corresponds to C–O stretching in fruit extract.

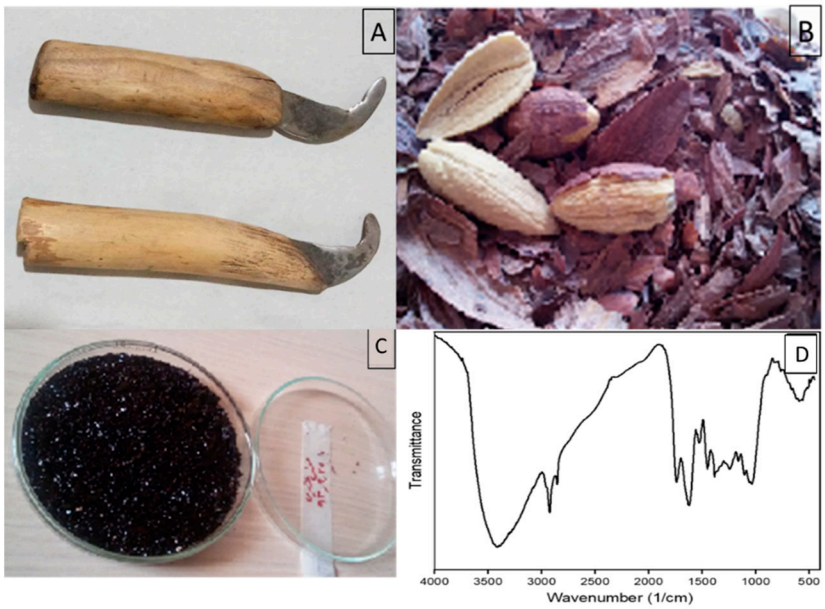

Figure 9. (**A**): Ronjok, (**B**): *Oak fruit*, (**C**): Jaft, and (**D**): the aqueous extract of *Oak fruit*.

3.5. Antioxidant Activity

The DPPH radical scavenger assay is widely used to assess the antioxidant capacity of various plant extracts and natural products [26]. This process relies on the ability of DPPH radicals to react with hydrogen donor species such as phenols and flavonoids in the extracted material. Upon receiving an H^+ from the donor species, they lose their color and turn yellow. As the concentration of phenolic compounds increases, so does their DPPH radical scavenging activity. A 1.0 mL of methanolic solution of DPPH (0.1 mM) in 3 mL methanol was mixed (containing 2–25 mg of the dried extract). The solution was vortexed and then incubated for 30 min at room temperature in the dark. Absorbance was measured at 515 nm and the activity was expressed as a percentage of DPPH uptake

relative to the control samples. The inhibition rate of DPPH free radicals was determined using the following formula:

$$\% \text{ inhibition} = [(Ac - As)/Ac] \times 100$$

Ac: absolute Blank

As: sample or standard absorption

IC_{50} or 50% inhibitory concentration was also calculated. IC_{50} is the maximum extract concentration that inhibits free radicals' activity or damage by 50%.

The superior DPPH radical scavenging ability results of extract prepared by UAE may be due to the presence of high concentration of phenolic through (Table 6).

Table 6. Calibration data of antioxidant activity assay by DPPH and phenolic standard by Folin Ciocalteu reagent.

Standard	Calibration (mg/mL^{-1})	IC50 ± SD
DPPH	Y = 46.124 x + 8.6987	61.7 ± 0.04

3.6. Antimicrobial Susceptibility Testing Method

3.6.1. Antibiotic Sensitivity of *H. pylori* Strains

Sensitive and resistance testing of bacteria was carried out by disk diffusion method. Firstly, we prepared Muller Hinton agar that was enriched with defibrinate sheep red blood cell 7%, then 10 mg of *H. pylori* suspensions equivalent to McFarland's turbidity well NO.3 and cultured on this media. Some standard antibiotics such as Amoxicillin (25 mcg), Tetracycline (30 mcg), Metronidazole (5 mcg), and Clarithromycin (15 mcg), were placed on this medium and incubated for 5 days under microaerophilic conditions and the zone of inhibition diameter measurement of the halo around the discs was read and recorded according to NCCLS standards (Table 7) [27].

Table 7. Antibiotic sensitivity for *H. pylori* strains.

Antibiotics	Sensitive		Intermediate		Resistant	
	Number	Percent	Number	Percent	Number	Percent
Amoxicillin (25 mcg)	39	74%	-	-	14	26%
Tetracycline (30 mcg)	43	81%	3	6%	7	13%
Metronidazole (5 mcg)	4	7%	-	-	49	92%
Clarithromycin (15 mcg)	37	70%	6	11%	10	19%

3.6.2. The Termination of the Zone of Inhibition for an Extract of *Oak fruit* and Blue-Light-Driven Photocatalyst

To measure the antimicrobial effect, the bacteria were cultured on campylobacter media plates (McFarland Standard No. 3) separately. For this proposed five standard discs (6mm) were selected. Number one contained 20mg of MIC concentration of extracted *Oak fruit*, No. 2 included 20mg of MIC concentration of $Bi_2WO_6/Ag_3PO_4/Ag$, and No. 3 contained 20mg of MIC concentration of $Bi_2WO_6/Ag_3PO_4/Ag$ and extracted of *Oak fruit* simultaneously.

3.6.3. Effectiveness of Bactericidal Performance of an Extract of *Oak fruit* and Blue-Light-Driven Photocatalyst

Under the conditions of Blue-Light-Driven photocatalyst, the minimal inhibitory concentration (MIC) was determined. The MIC is the lowest concentration of a substance that can prevent bacterial growth, and bacteria can regrow once the antimicrobial is removed from the

medium. The MIC of *Oak fruit* extracts was determined using the broth microdilution method in 96-well microplates, based on CLSI (Clinical and Laboratory Standards Institute) guidelines. In this experiment, the total amount of antibacterial, bacteria, and the medium in each well was 100 mg and the number of bacteria in the well was 5×10^5 CFU/mL. $Bi_2WO_6/Ag_3PO_4/Ag$ was then added to the wells at dilutions of 200−0.38 mg/mL to the wells. One row of wells was considered a positive control (no antibacterial agent, bacterial growth) and another row was considered a negative control (no bacteria). The Treatments-containing wells were inoculated following overnight incubation for 72 h at 37 °C in microaerophilic conditions. Also, another row was used as the negative control, including substances without bacteria. All tests were repeated three times. The wells were examined for visible bacterial growth as evidenced by turbidity. Then, all wells' absorbance was measured by an ELISA reader at 650 nm according to the following equation:

$$\text{Percentage of inhibition} = (1 - a/b) \times 100$$
$$a: \text{ absorbance of treated wells}$$
$$b: \text{ absorbance of control}$$

To determine the minimum bactericidal concentration, all non-opaque wells from MIC experiments were cultured on a blood agar culture medium and placed in an incubator for 18–24 h before examining the culture media. The lowest concentration of *Oak fruit* extract at which bacteria did not grow, 99.9%, was reported as MBC [24,25].

3.7. Treatment of H. pylori with Photocatalyst under the Conditions of Blue-Light-Driven Photocatalyst and Oak fruit Extract

For proofing, the photocatalytic bactericidal effects of $Bi_2WO_6/Ag_3PO_4/Ag$ were studied on the expression of the *urease gene* in the standard and clinical *H. pylori*. Hence, gastric biopsy specimens were ground at 10,000 rpm for 15 s with an electric tissue homogenizer (Ultraturrax, Iena, Germany) and then incubated onto selective Columbia blood agar and incubated under microaerophilic (5% oxygen, 10% carbon dioxide, and 85% nitrogen) conditions at 37 °C for up to seven days [21,22]. Then, to investigate the effect of $Bi_2WO_6/Ag_3PO_4/Ag$ photocatalyst on the expression of *H. pylori's urease gene* samples were treated with MIC amount of $Bi_2WO_6/Ag_3PO_4/Ag$ and, after that, used for molecular works. The 400 mg of $Bi_2WO_6/Ag_3PO_4/Ag$ has put into the 100 mL bacteria suspension 1.5×10^8 CFU/mL) and transferred in microplates for photocatalytic disinfection experiments. Latterly, 100 µL suspension was taken out every two hours during the photocatalytic experiments, and spread on agar medium and cultured at 37 °C for 20 h to achieve the number of alive bacteria after photocatalytic disinfection. On the other side experiment in the absence of light was completely resolute with the conditions in the visible-blue light.

To study the effect of *Oak fruit* extract on *urease gene* expression considering MIC, *H. pylori* samples were first treated with *Oak fruit* extract. Next, we extracted and examined the bacterial RNA. For this purpose, the volume required for sedimentation according to MIC for 1.0 mL of microcells was calculated using the formula $C_1V_1 = C_2V_2$. After calculation, the volume needed for each treatment and 50 mg of bacteria at a concentration of 10^7 CFU/mL was poured into 1.5 mL microwells. The remaining volume was then made up to 1.0 mL with sterile Muller Hinton broth medium and incubated at 37 °C for 18–24 h before samples were used for RNA extraction [28].

3.8. RNA Extraction and cDNA Preparation

The extracted RNA was measured from various samples including the clinical and standard microbial, following the manufacturer's instructions using the RNase/mini kit for bacterial cells (Bioflux, Japan product, Tokyo, Japan). The residue from the prior step and the concentration of RNA extracted with the nanodroplet device was stored at −70 °C. RNA extracted from the samples was combined using a DNase material (Thermo Scientific) that destroys the DNA within the samples leaving only the RNA (all materials were added to an RNase-free micrometry). The compounds used in the DNase are: 1 mg RNA (10) × reaction

buffer with $MgCl_2$ at 1 mg concentration, DNase and RNase free with 1 mg concentration. The DEPC-treated water was used at a concentration of 10 mg, then the material was incubated in the microtip at 37 °C for 30 min. Finally add 1 mg EDTA (50 mM) and incubate at 10 °C for 65 min. cDNA synthesis was carried out in two steps, cDNA synthesis and PCR, using, prime script reagent kit (Takara). First, the extracted RNA was removed from the freeze-dried condition at −70 °C under sterile conditions and then placed on ice. A master mix was prepared on ice, split into the microtips; finally, the RNA extracted from each sample was added to a microtip. Ready-to-use samples were to a thermal cycler. At this stage cDNA was generated in two different temperature range cycles. In the final step, samples were brought to a freezing temperature of −20 °C under sterile conditions [29].

3.9. Real-Time PCR

Real-time PCR analysis was executed on a Rotor-Gene 6000 (Corbett Research, Sydney, Australia). In summary, the 25 mL PCR mixture includes two milliliters of extracted DNA, 200 mM dNTPs (CinnaGen, Co., Tehran, Iran), 0.2 mM (each) primer HP23S-1 and HP23S-2, 0.1 mM probe Pwt, 0.2 mM (each) primer HP-1 and HP-2 0.1 mM probe Pwt, 16S rRNA, (Bioneer, Daejeon, Korea), 1.5 mM $MgCl_2$, and 1.5 U of Taq polymerase in PCR buffer (CinnaGen, Co., Tehran, Iran), was denatured at 95 °C for five min; amplification was carried out in 45 cycles of 95 °C for 30 s and 58 °C for 40 s. Study of fluorescence for each sample was taken during the annealing steps on various channels. Total tests were taken twice, including positive and negative controls in each assay. Data analysis is done with instrument-compliant software (ver1.7; Corbett Research, Sydney, Australia). Primer's specificity test of the primers with purified DNA from non-*H. pylori* bacterial strains as a template were used. The cycle threshold (Cq) value was determined for every channel as the number of cycles at which fluorescence exceeded the threshold limit, set at the top of the second derivative fluorescence curve and expressed as fractional cycle numbers.

3.9.1. PCR to Confirm Urease Gene

The *urease gene* is confirmed through the kit of Sin a gene Company and Corbett thermocycler of America refer to Table 8.

Table 8. The sequence of used primers to determine Urease gene.

Target (Reference), Nucleotide (nt) Positions Amplified, and Size of PCR Products	Primer Names and Sequences	PCR Conditions (One Minute)
urease gene [26], nt 304–714, 411 bp	Urease, 5′-GCCAATGGTAAATTAGTT-3′ Urease, 5′-CTCCTTAATTGTTTTTAC-3′	94 °C; 45 °C; 72 °C (38 cycles)

3.9.2. Sample Preparation for PCR Amplification

PCR targeting the 16S rRNA gene was carried out to confirm *H. pylori* in every sample. Preformation of different microbial samples such as, clinical and standard RNA extraction was done by the producer's directions using the RNase/mini kit for bacterial cells (bioflux, Japan product) from the earlier step sediment and the Nano-droplet device measured the concentration of extracted RNA and stored in −70 °C. The sequence and temperature of melting of the studied genes (HP-1, HP-2) are shown in Table 9 [27]. PCR amplification of genomic DNA was executed in a reaction consisting of a 25 mL mixture including 2 mL biopsy-isolated DNA template, 1.5 mM $MgCl_2$, 0.2 mM deoxynucleotide triphosphates (dNTPs) mixture, 0.2 mM of each primer, and 1 U of Taq DNA polymerase (CinnaGen, Co., Tehran, Iran). The thermal-cycling conditions were performed as follows: initial denaturation at 95 °C for five minutes; 30 cycles of 95 °C for a minute, 58 °C for one minute and 72 °C for one minute; and a final extension at 72 °C for five minutes. The resulting Hp16S fragment (expected size of 109 base pairs) was embodied after electrophoresis on a 1.5% agarose gel stained with ethidium bromide.

Table 9. Oligonucleotide sequences used in this study.

Target (Reference), Nucleotide (nt) Positions Amplified, and Size of PCR Products	Primer Names and Sequences	PCR Conditions (One Minute)
16S rRNA [27] nt 635–744, 110 bp	Hp-1, 5′- CTGGAGAGACTAAGCCCTCC-3′	95 °C; 58 °C; 72 °C, (30 cycles)

4. Conclusions

In conclusion, the obtained results from the *Oak fruit* extract as a natural disinfectant showed significant antibacterial properties, and it acted as an antibacterial substance on biopsy samples from *H. pylori* bacteria under clinical and standard conditions. In addition, the antibacterial photocatalytic activity of the previously reported Z-scheme $Bi_2WO_6/Ag_3PO_4/Ag$ plasmonic heterojunction driven blue-light photocatalyst for a novel application was studied, and the results supported the antibacterial efficiency of the photocatalyst under blue light for *H. pylori* bacteria disinfection. This research opens new insights into disinfectants against bacteria as well as a proposed photocatalyst for easily removing *H. pylori* bacteria from contaminated environments.

Author Contributions: Conceptualization, M.A., K.D. and F.A.; Methodology, M.A., S.A. and A.A.; Software, K.D. and V.P.; Validation, K.D. and V.P.; Formal analysis, K.D.; Investigation K.D. and V.P.; Resources, S.A.K.; Data curation, K.D. and V.P.; Writing—original draft preparation, K.D., V.P. and F.A.; Writing—review and editing, K.D. and F.A.; Visualization, F.A.; Supervision, M.G. and A.S; Project administration, K.D. and V.P.; Funding acquisition, M.G., A.S. and G.Y. All authors have read and agreed to the published version of the manuscript.

Funding: This research was funded by Yasuj University of Medical Sciences and Yasouj University: 6b4d75613f66244a.

Acknowledgments: The authors are grateful to Yasuj University of Medical Sciences, Iran, for the financial support of this work. We also sincerely appreciate the significant contributions made by the Azizi clinical laboratory, the Dena pathobiology laboratory, and Yasouj University, (Yasouj, Iran).

Conflicts of Interest: The authors declare no conflict of interest.

References

1. Liburd, L.C.; Hall, J.E.; Mpofu, J.J.; Williams, S.M.; Bouye, K.; Penman-Aguilar, A. Addressing health equity in public health practice: Frameworks, promising strategies, and measurement considerations. *Annu. Rev. Public Health* **2020**, *41*, 417–432. [CrossRef] [PubMed]
2. Nowacka, M.; Rygała, A.; Kręgiel, D.; Kowalewska, A. Poly (silsesquioxanes) and poly (siloxanes) grafted with N-acetylcysteine for eradicating mature bacterial biofilms in water environment. *Colloids Surf. B Biointerfaces* **2018**, *172*, 627–634. [CrossRef] [PubMed]
3. Tortajada, C.; van Rensburg, P. *Drink More Recycled Wastewater*; Nature Publishing Group: London, UK, 2020.
4. Kumar, R.; Raizada, P.; Verma, N.; Hosseini-Bandegharaei, A.; Thakur, V.K.; Van Le, Q.; Nguyen, V.-H.; Selvasembian, R.; Singh, P. Recent advances on water disinfection using bismuth based modified photocatalysts: Strategies and challenges. *J. Clean. Prod.* **2021**, *297*, 126617. [CrossRef]
5. Šterbenc, A.; Jarc, E.; Poljak, M.; Homan, M. Helicobacter pylori virulence genes. *World J. Gastroenterol.* **2019**, *25*, 4870. [CrossRef] [PubMed]
6. Graham, D.Y.; Miftahussurur, M. Helicobacter pylori urease for diagnosis of Helicobacter pylori infection: A mini review. *J. Adv. Res.* **2018**, *13*, 51–57. [CrossRef]
7. Priyadarsini, S.; Mukherjee, S.; Bag, J.; Nayak, N.; Mishra, M. Application of nanoparticles in dentistry: Current trends. In *Nanoparticles in Medicine*; Springer: Berlin/Heidelberg, Germany, 2020; pp. 55–98.
8. Amiri, M.; Dashtian, K.; Ghaedi, M.; Mosleh, S.; Jannesar, R. Bi_2WO_6/Ag_3PO_4–Ag Z-scheme heterojunction as a new plasmonic visible-light-driven photocatalyst: Performance evaluation and mechanism study. *New J. Chem.* **2019**, *43*, 1275–1284. [CrossRef]
9. Razaghi, P.; Dashtian, K.; Yousefi, F.; Karimi, R.; Ghaedi, M. Gold anchoring to $CuFe_2F_8(H_2O)_2$ oxyfluoride for robust sono-photodegradation of Rhodamine-B. *J. Clean. Prod.* **2021**, *313*, 127916. [CrossRef]
10. Zhao, W.; Zhang, J.; Zhu, F.; Mu, F.; Zhang, L.; Dai, B.; Xu, J.; Zhu, A.; Sun, C.; Leung, D.Y. Study the photocatalytic mechanism of the novel Ag/p-Ag_2O/n-$BiVO_4$ plasmonic photocatalyst for the simultaneous removal of BPA and chromium (VI). *Chem. Eng. J.* **2019**, *361*, 1352–1362. [CrossRef]

11. Liu, Y.; Kong, J.; Yuan, J.; Zhao, W.; Zhu, X.; Sun, C.; Xie, J. Enhanced photocatalytic activity over flower-like sphere $Ag/Ag_2CO_3/BiVO_4$ plasmonic heterojunction photocatalyst for tetracycline degradation. *Chem. Eng. J.* **2018**, *331*, 242–254. [CrossRef]
12. Dashtian, K.; Shahbazi, S.; Tayebi, M.; Masoumi, Z. A review on metal-organic frameworks photoelectrochemistry: A headlight for future applications. *Coord. Chem. Rev.* **2021**, *445*, 214097.
13. Wen, X.-J.; Niu, C.-G.; Zhang, L.; Liang, C.; Guo, H.; Zeng, G.-M. Photocatalytic degradation of ciprofloxacin by a novel Z-scheme CeO_2–Ag/AgBr photocatalyst: Influencing factors, possible degradation pathways, and mechanism insight. *J. Catal.* **2018**, *358*, 141–154. [CrossRef]
14. Shamloufard, A.; Hajati, S.; Youzbashi, A.; Dashtian, K.; Moradi, M.; Toth, J. S-scheme NIR-edge Ag3CuS2/VO2 heterostructure for photo-oxidation/reduction of methylene blue/Cr (VI). *Appl. Surf. Sci.* **2022**, *590*, 153118. [CrossRef]
15. Adeeyo, A.O.; Edokpayi, J.N.; Alabi, M.A.; Msagati, T.A.; Odiyo, J.O. Plant active products and emerging interventions in water potabilisation: Disinfection and multi-drug resistant pathogen treatment. *Clin. Phytoscience* **2021**, *7*, 31. [CrossRef]
16. Saquib, S.A.; AlQahtani, N.A.; Ahmad, I.; Kader, M.A.; Al Shahrani, S.S.; Asiri, E.A. Evaluation and comparison of antibacterial efficacy of herbal extracts in combination with antibiotics on periodontal pathobionts: An in vitro microbiological study. *Antibiotics* **2019**, *8*, 89. [CrossRef] [PubMed]
17. Aidy, A.; Bahmani, M.; Pirhadi, M.; Kaviar, V.H.; Karimi, E.; Abbasi, N. Phytochemical Analysis and Antimicrobial Effect of Essential Oil and Extract of Loranthus europaeus Jacq. on Acinetobacter baumannii, Staphylococcus aureus, and Pseudomonas aeruginosa. *Kafkas Univ. Vet. Fak. Derg.* **2022**, *28*, 26626.
18. Dehelean, C.A.; Marcovici, I.; Soica, C.; Mioc, M.; Coricovac, D.; Iurciuc, S.; Cretu, O.M.; Pinzaru, I. Plant-derived anticancer compounds as new perspectives in drug discovery and alternative therapy. *Molecules* **2021**, *26*, 1109. [CrossRef]
19. Salehi, B.; Sharopov, F.; Martorell, M.; Rajkovic, J.; Ademiluyi, A.O.; Sharifi-Rad, M.; Fokou, P.V.T.; Martins, N.; Iriti, M.; Sharifi-Rad, J. Phytochemicals in Helicobacter pylori infections: What are we doing now? *Int. J. Mol. Sci.* **2018**, *19*, 2361. [CrossRef]
20. Naseri, H.; Sharifi, A.; Ghaedi, M.; Dashtian, K.; Khoramrooz, S.S.; Manzouri, L.; Khosravani, S.A.; Pezeshkpour, V.; Sadri, F.; Askarinia, M. Sonochemical incorporated of cytosine in Cu-H2bpdc as an antibacterial agent against standard and clinical strains of Proteus mirabilis with rsbA gene. *Ultrason. Sonochem.* **2018**, *44*, 223–230. [CrossRef] [PubMed]
21. Opekun, A.R.; Zierold, C.; Rode, A.; Blocki, F.A.; Fiorini, G.; Saracino, I.M.; Vaira, D.; Sutton, F.M. Clinical performance of the automated LIAISON®meridian *H. pylori* SA stool antigen test. *BioMed Res. Int.* **2020**, *2020*, 7189519. [CrossRef]
22. Mwinyikombo, I.S. *Isolation, Antibiotic Susceptibility and Molecular Characterisation of Resistance Genes in Pseudomonas Isolates from Selected Hospitals in Mombasa County*; Kenyatta University: Nairobi, Kenya, 2018.
23. Ghotaslou, R.; Pirzadeh, T.; Esmailkhani, A.; Bialvaei, A.Z.; Leylabadlo, H.E. Recent advances in the diagnosis of Helicobacter pylori infection. *J. Sabzevar Univ. Med. Sci.* **2022**, *29*, 179–194.
24. Rey, L. Revista do Instituto de Medicina Tropical de São Paulo (Journal of the São Paulo Institute of Tropical Medicine) fifty years later. *Rev. Inst. Med. Trop. São Paulo* **2009**, *51*, 239–240. [CrossRef] [PubMed]
25. De Sotillo, D.R.; Hadley, M.; Holm, E. Phenolics in aqueous potato peel extract: Extraction, identification and degradation. *J. Food Sci.* **1994**, *59*, 649–651. [CrossRef]
26. Yang, J.; Chen, J.; Hao, Y.; Liu, Y. Identification of the DPPH radical scavenging reaction adducts of ferulic acid and sinapic acid and their structure-antioxidant activity relationship. *LWT* **2021**, *146*, 111411. [CrossRef]
27. Zou, Y.; Qian, X.; Liu, X.; Song, Y.; Song, C.; Wu, S.; An, Y.; Yuan, R.; Wang, Y.; Xie, Y. The effect of antibiotic resistance on Helicobacter pylori eradication efficacy: A systematic review and meta-analysis. *Helicobacter* **2020**, *25*, e12714. [CrossRef]
28. Abbasloo, F.; Khosravani, S.A.; Ghaedi, M.; Dashtian, K.; Hosseini, E.; Manzouri, L.; Khorramrooz, S.S.; Sharifi, A.; Jannesar, R.; Sadri, F. Sonochemical-solvothermal synthesis of guanine embedded copper based metal-organic framework (MOF) and its effect on oprD gene expression in clinical and standard strains of Pseudomonas aeruginosa. *Ultrason. Sonochem.* **2018**, *42*, 237–243. [CrossRef]
29. Musini, A.; Chilumoju, S.P.; Giri, A. Biofilm Formation in Drug-Resistant Pathogen Staphylococcus aureus. In *Microbial Biofilms*; CRC Press: Boca Raton, FL, USA, 2022; pp. 23–46.